Journal of Hydrology: Regional Studies 35 (2021) 100826

Contents lists available at ScienceDirect

Journal of Hydrology: Regional Studies

journal homepage: www.elsevier.com/locate/ejrh

Impacts of swat weather generator statistics from high-resolution datasets on monthly streamflow simulation over Peninsular Spain

Javier Senent-Aparicio [a,*], Patricia Jimeno-Sáez [a], Adrián López-Ballesteros [a], José Ginés Giménez [b], Julio Pérez-Sánchez [a], José M. Cecilia [c], Raghavan Srinivasan [d]

[a] Department of Civil Engineering, Catholic University of Murcia (UCAM), Murcia, Spain
[b] Department of Computer Engineering, Catholic University of Murcia (UCAM), Murcia, Spain
[c] Department of Computer Engineering, Universitat Politécnica de Valencia (UPV), Valencia, Spain
[d] Department of Ecosystem Science and Management, Spatial Sciences Laboratory, Texas A&M University, College Station, TX, United States

ARTICLE INFO

Keywords:
Weather generator
CFSR
SWAT
Peninsular Spain

ABSTRACT

Study region: Peninsular Spain.
Study focus: Weather data are the key drivers of hydrological modelling. However, available weather data can present gaps in data sequences and are often limited in their spatial coverage for use in such hydrological models as the Soil and Water Assessment Tool (SWAT). To overcome this limitation, SWAT includes a weather generator algorithm that can complete this data based on long-term weather statistics. This work presents a newly developed weather statistics dataset for Peninsular Spain (PSWG), calculated from national gridded datasets according to the SWAT model format. PSWG provides a higher resolution that stands as a compelling alternative to the statistics calculated from the Climate Forecast System Reanalysis (CFSR) that are available on the SWAT website.
New hydrological insights for the region: The dataset has been evaluated using PSWG and CFSR datasets for different data availability scenarios to reconstruct weather series in three watersheds with contrasting weather climates. Results underscore the superiority of the PSWG dataset in reconstructing missing data for hydrological simulations. This approach provides a strong alternative for SWAT applications in Peninsular Spain and the applied methodology can be replicated in other countries that dispose of high-resolution gridded rainfall and temperature datasets.

1. Introduction

Meteorological data is crucial in the application of hydrological models such as the Soil and Water Assessment Tool (SWAT) (White et al., 2017). The SWAT model is an eco-hydrological public domain model with a physical and semi-distributed base, which works in a daily time step, and has been widely applied in hydrological and environmental studies, due to its capacity to simulate different hydrological processes (Arnold et al., 1998). SWAT is the most widely used watershed-scale water quality model in the world (Tan et al., 2020) and its use in Spain is also widespread. Over the last 3 years, we find numerous studies in Spanish watersheds related to the study of hydrological and water quality processes (Jimeno-Sáez et al., 2018; Malik et al., 2020; Rivas-Tabares et al., 2019; Senent-Aparicio et al., 2020, 2019), the impact of climate change (Meaurio et al., 2017; Pérez-Sánchez et al., 2020; Senent-Aparicio et al.,

* Corresponding author.
E-mail address: jsenent@ucam.edu (J. Senent-Aparicio).

https://doi.org/10.1016/j.ejrh.2021.100826
Received 1 January 2021; Received in revised form 27 March 2021; Accepted 24 April 2021
Available online 5 May 2021

2017), or the impact of human pressures on water resources (Cánovas et al., 2018; Essenfelder et al., 2018; Jodar-Abellan et al., 2019; López-Ballesteros et al., 2019; Peraza-Castro et al., 2018; Salmoral et al., 2017; Senent-Aparicio et al., 2018a).

Observed weather data are often inadequate, in terms of completeness, length, and spatial coverage, which accounts for the need to use weather generators that solve this problem by generating data with the same statistical properties as the observed data (Vesely et al., 2019). SWAT includes a weather generator module (WGEN) that can fill in missing weather data and simulate weather parameters for which observed data are not available (Richardson, 1981). This WGEN requires monthly parameters of rainfall (average, standard deviation, skewness, sequences of wet or dry days), temperature (maximum, minimum, dew point), wind speed and solar radiation (Neitsch et al., 2011). As do other weather generators, WGEN depends strongly on rainfall data, as half of the WGEN required statistics are related to rainfall.

Obtaining and processing meteorological data for hydrological modelling is time-consuming and susceptible to errors (Abbaspour et al., 2019). SWAT developers, to help SWAT users, have included on their website (SWAT, 2020) the option to download global weather daily data (precipitation, maximum and minimum temperature, wind speed, solar radiation and relative humidity) from the Climate Forecast System Reanalysis (CFSR) (Saha et al., 2010) in SWAT file format for a given location and time period. In addition, SWAT also provides a database file that includes all weather statistical data needed for the operation of the WGEN. The time-saving nature of this database means that it is extensively used by SWAT users (Ghimire et al., 2019). CFSR weather data have also been used to force SWAT for several different watersheds around the world and many recent studies agree on the weak performance in the simulation of daily and monthly streamflows (Duan et al., 2019; Gao et al., 2018; Meng et al., 2019; Roth and Lemann, 2016; Tan et al., 2017; Thom et al., 2017; Zhu et al., 2016).

Several studies have recently evaluated the performance of different weather generators for hydrological modelling with the SWAT model. Alodah and Seidou (2019) evaluated five different weather generators concluding that the WGEN called MulGETS (Chen et al., 2014) showed the best performance. Chen et al. (2019) adjusted the daily rainfall ad temperature time series generated by MulGETS using monthly and annual climate time series generated by a first-order linear autoregressive model. Dai and Qin (2019) assessed the effectiveness of a multi-site stochastic WGEN on hydrological responses in the Red Deer River watershed, Canada. The results indicated that multi-site generators were capable of better representing the monthly streamflow variability. Yang et al. (2020) integrated an hourly WGEN with an hourly SWAT model whose performance indicated that it could reasonably characterise the main monthly, daily, and hourly rainfall features. However, to our knowledge, only Ghimire et al. (2019) have dealt with the influence of the input data used to calculate the statistics required for the application of the SWAT WGEN for hydrological simulations. They developed a comprehensive dataset for the Asia Pacific region that clearly enhanced the widespread use of CFSR data among the SWAT community. In Europe and therefore in Spain there is no previous precedent, so the development of the dataset presented in this study can help to a more accurate simulation of the hydrological processes in Peninsular Spain.

In recent years, two high-resolution gridded datasets have been developed in Spain that can be very useful in hydrological modelling. The Spain02 project (Herrera et al., 2016) includes daily rainfall and maximum and minimum temperature data covering Peninsular Spain and at a resolution of 0.1° (≈10 km) from 1950 to 2015. This project has been successfully applied in the modelling of different Spanish basins (Baena-Ruiz et al., 2020; Pérez-Sánchez et al., 2020; Pulido-Velazquez et al., 2018b, 2018a; Rupérez-Moreno et al., 2017; Senent-Aparicio et al., 2018a, 2017). More recently, the Spanish National Meteorological Agency (AEMET) developed a high-resolution (5 km) precipitation (Peral-García et al., 2017) and temperature gridded dataset (Amblar-Francés et al., 2020) for the period of 1951 to the present over Spain. The Spain02 and AEMET grids were generated by interpolation of observed data. Recent studies compared different gridded rainfall products over Peninsular Spain and concluded that the national AEMET gridded dataset was superior to the other rainfall remote sensing products (Senent-Aparicio et al., 2018b). These results suggest that the AEMET dataset may be a better alternative for the estimation of precipitation statistics needed for the SWAT WGEN file. Thus, the aim of our work is threefold: (1) to develop an accurate meteorological dataset ready for use in the SWAT model that combines rainfall and temperature weather statistics from AEMET, and other weather statistics related with the wind speed, solar radiation, and relative humidity from CFSR, hereinafter called Peninsular Spain Weather Generator Dataset (PSWG); (2) to calculate all statistics that are needed to run SWAT WGEN throughout Peninsular Spain and (3) to assess the performance of the statistics computed using the PSWG dataset over the existing CFSR dataset in a streamflow simulation for different weather conditions in Peninsular Spain.

2. Materials and methods

Fig. 1 shows the general approach taken to obtain the PSWG dataset. The following sections elaborate on the independent data sources used as inputs, how these inputs were combined, and the methods used to calculate all the statistics included in the PSWG dataset in greater detail. Step 3 in Fig. 1 shows the evaluation and impact of using PSWG data in a flow simulation with the SWAT model.

2.1. Extraction and combination of daily weather data to generate the PSWG dataset

2.1.1. Input daily weather data

The various data sources used as input data are presented in Table 1. Daily precipitation for the period 1951–2019 was obtained from the AEMET gridded dataset v2, with a 5 km resolution (Peral-García et al., 2017). This dataset was developed on the basis of over 2300 rainfall stations and is available in netcdf format at the AEMET climate services website (AEMET, 2020). Related to humidity, wind speed, and solar radiation, these weather variables were extracted from CFSR (Saha et al., 2010). This global reanalysis dataset is extensively used as source of meteorological data and is offered free-access on the official website of the SWAT model (SWAT, 2020) in

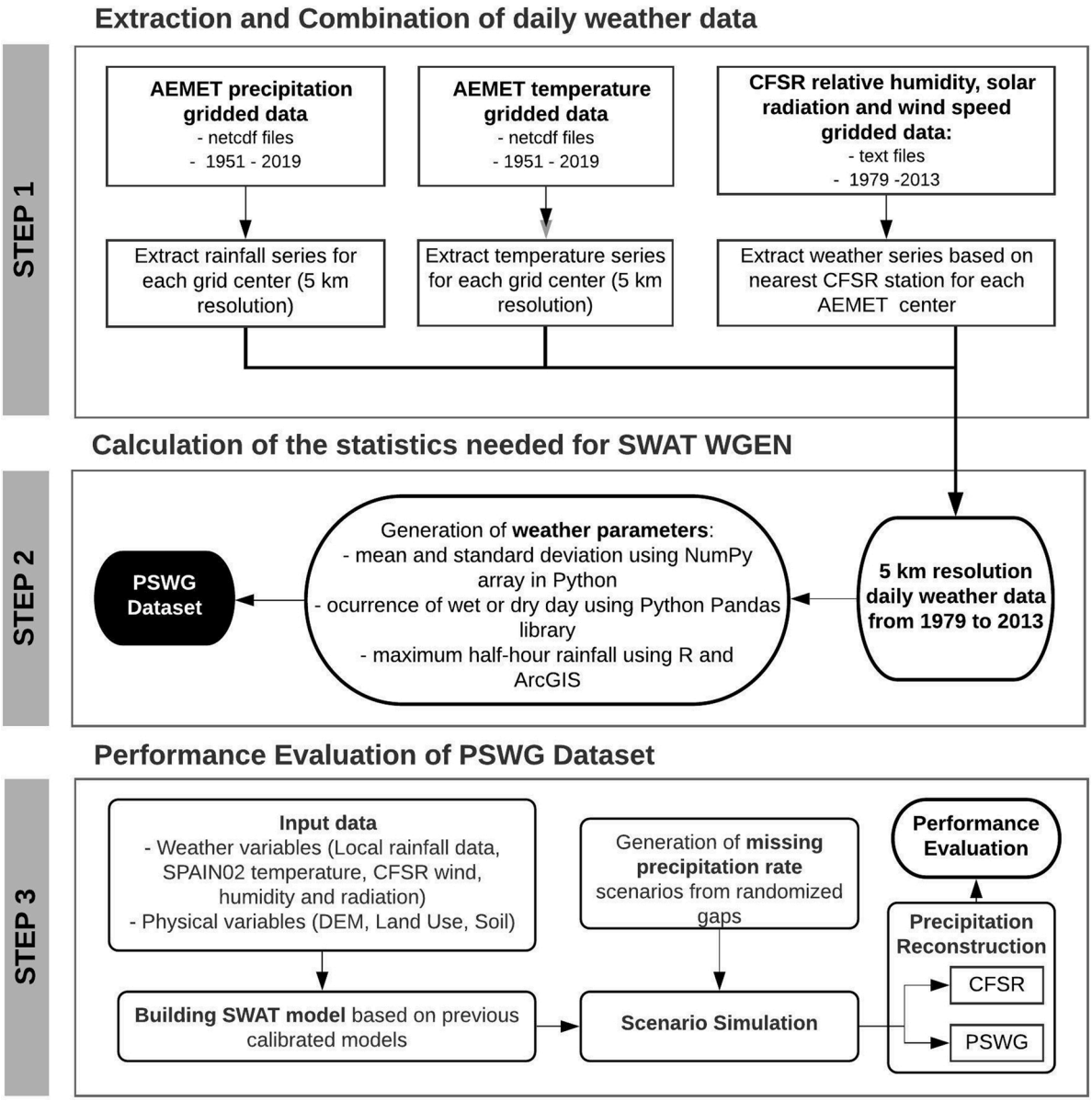

Fig. 1. Schematic figure of the approach to generating the PSWG dataset for Peninsular Spain.

Table 1
Main characteristics of the input data sources used to obtain PSWG.

Variable	Source	Resolution	Temporal Coverage
Rainfall Temperature	AEMET	5 km	1951 – 2019
Wind speed Solar radiation Relative humidity	CFSR	38 km	1979–2013

SWAT-ready format. This interpolated dataset was created by the National Centers for Environmental Prediction (NCEP) and is based on hourly forecasts derived using from satellite product information and the global weather station network. CFSR datasets are available from 1979 to 2013 with a resolution of 38 km.

2.1.2. Combination of datasets

Before calculating WGEN statistics, it was necessary to extract the information for each of the grid centres of AEMET's 5 km grid.

MATLAB scripts were used to extract this information (MATLAB, version R2013b) and to extract SPAIN02 temperature data. CFSR data were directly downloaded for each of the grid centres from the SWAT website. To assign temperature, wind speed, solar radiation, and humidity values to the 5 km grid, ArcGIS was used to identify the nearest SPAIN02 and CFSR station for each AEMET centre. Final datasets were imported into a PostgresSQL (PostgreSQL, 2020) database, designed to provide faster data analysis in further analysis. The database scheme has a table for each station, with such properties as coordinates and elevation. There is also a table for each weather variable: temperature, precipitation, wind, etc., which save in each row the related measures (e.g. Temperature table has MAX and MIN), date and station.

From the database, we can easily select the common period 1979–2013 to analyse in this work. This period of time (35 years) is sufficiently long, given that, according to SWAT Input/Output documentation (Arnold et al., 2012), more than 20 years of data are needed to calculate the statistical data needed to represent daily weather data.

2.2. Calculation of the WGEN statistics

SWAT includes a built-in WGEN, developed by Sharpley and Williams (1990), to generate weather data that is not available or to complete gaps in observed measurements. This WGEN requires monthly parameters of skewness, standard deviation, and average rainfall, maximum half-hour rainfall for each month, probability of occurrence of dry or wet days, mean and standard deviation of temperatures, solar radiation, and wind speed. WGEN first independently determines the day's precipitation. A first-order Markov chain is used to determine whether the day is dry or wet, which means that it takes into account the previous day's wet or dry condition (Schuol and Abbaspour, 2007). For each wet day, an exponential or skewed distribution is applied to generate the rainfall volume. Then, maximum and minimum temperature, solar radiation and relative humidity are generated, based on the presence or lack of rain for the day. Wind speed is generated on an independent basis. Details of WGEN equations are provided in SWAT theoretical documentation (Neitsch et al., 2011).

We use Python to obtain the data from the database and to get the WGEN parameter of the analysis. The Numpy (van der Walt et al., 2011) Python package provides 47 power mathematical functions to obtain skewness, standard deviations and means from a dataset. As some WGEN parameters represent monthly statistics among the selected years, the data frame must be grouped before applying the functions. The code below summarizes this part:

```
1 df = pds.read_sql("Select station, date, daily_accumulated from precipitation where station = 1 and date BETWEEN '1/1/1979' and '31/12/2013' Order by date asc", dbConnection)
2 df['date'] = pds.to_datetime(df['date'], format="%Y/%m/%d")
3 df.index = df['date']
4 df['month'] = df.index.month
5 analysis = df[['month','daily_accumulated']]
6 byMonth = analisis.groupby('month)
7 D['pcpstd'] = byMonth.std()
8 D['pcpskw'] = byMonth.skew()
```

Line 1 creates a data frame with the precipitation for station 1 between 1979 and 2013. Lines 2–4 define the data frame indexes. In this case, "date" is important, as we are working with time series. Moreover, the "month" index is important to group the values by month and then apply functions to them, such as mean, std, skew, (see lines 5–6). 'D' is a final data frame that contains the final

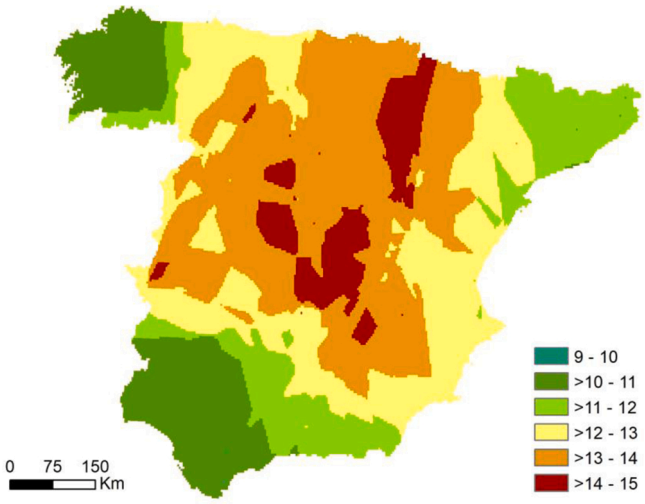

Fig. 2. Torrentiality index in Peninsular Spain during the period 1979-2013.

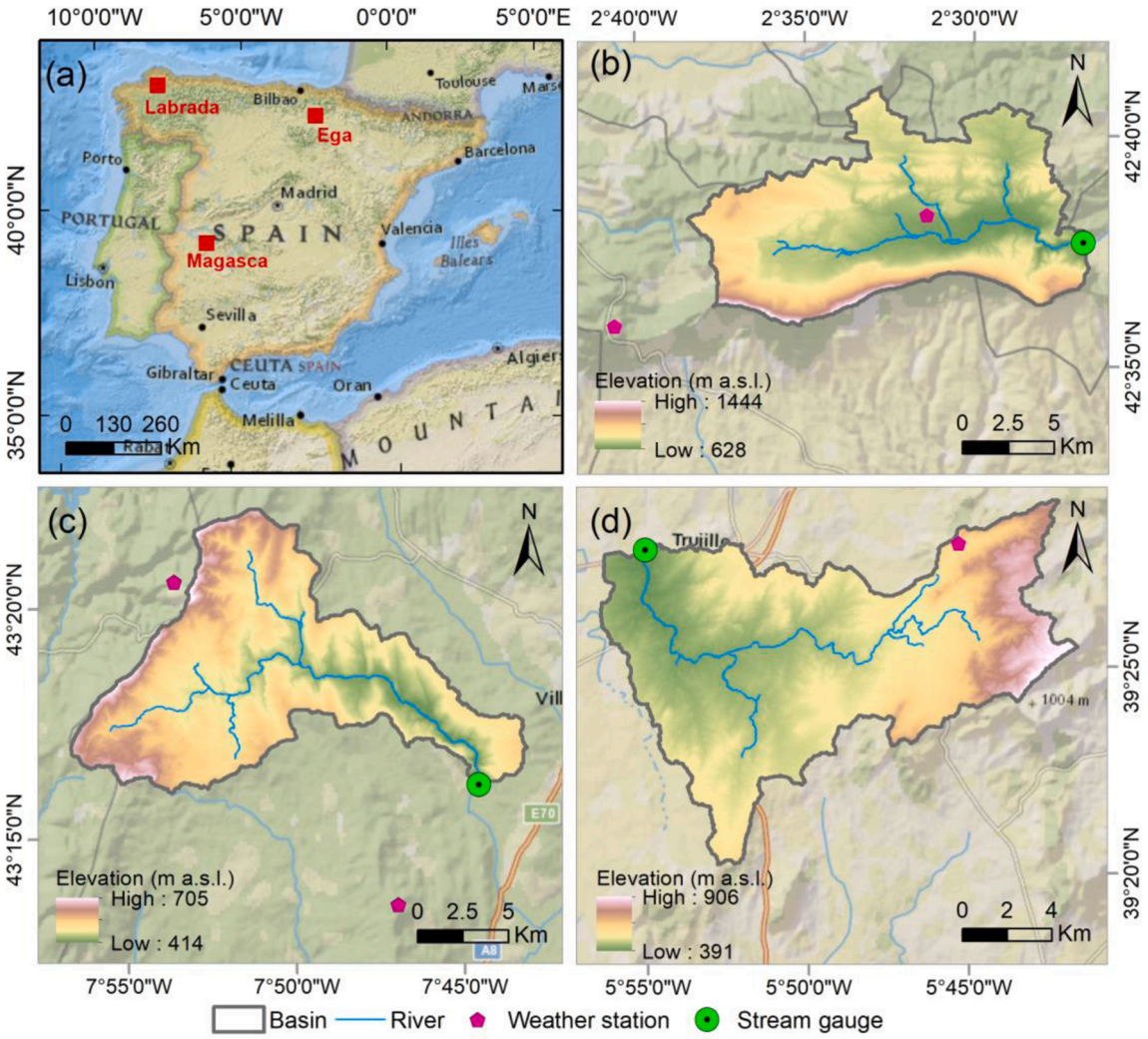

Fig. 3. **(a)** Location of the study areas in Peninsular Spain; **(b)** ERB; **(c)** LRB; **(d)** MRB.

Table 2
Summary of basins' characteristics. Obtained for the period October 2011 – September 2017.

Characteristic	LRB	MRB	ERB
Area (km^2)	95	165	89
Mean Elevation (m)	519	531	816
Mean annual precipitation (P) (mm)	1422	508	712
Mean annual potential evapotranspiration (PET) (mm)	784	1185	972
Köppen Climate	Csb	Csa	Cfb
Aridity Index (P/PET)	1.81	0.43	0.73
Mean annual flow (m^3/s)	2.81	0.47	0.79
Major Landuse (%)	Shrublands (34 %)	Natural Grasslands (25 %)	Forest (68 %)
Major Soil (%)	Humic Cambisols (82 %)	Dystric Regosols (64 %)	Rendzic Leptosols (53 %)

necessary WGEN statistics as the result of these processes. This 'D' data frame allows future exports, for example, to Microsoft Access. This process is like other monthly statistics, such as wind speed, dew point and solar radiation.

To obtain the occurrences of wet or dry days, we use Python Pandas library, which can manage data frame information. Using the Shift() data frame function, a value can be compared with the previous (or next) one in a temporal series. In this way, the auxiliary information can be obtained (i.e. "wet days followed by dry/wet days") needed for PR_W1 and PR_W2. To get the number of wet or dry days in a month, we apply the code explained before to group the data by month, then count the days with zero precipitation as dry and wet in other cases, as mentioned in the SWAT Input/Output documentation (Arnold et al., 2012).

The maximum rainfall of 30 min in the whole registration period for each month (RAINHHMX) is a difficult parameter to obtain, as

it is unusual to dispose of data on a sub daily scale for large scale watersheds. The CFSR database available on the SWAT website, and the SWAT Weather Database software (Essenfelder, 2018), also available on the SWAT website to create your own WGEN file, estimate RAINHHMX as the average of a third of the maximum recorded daily rainfall for that month. In our study, RAINHHMX was derived from the study of Moncho et al. (2009). In this work, the sub daily data from 64 rainfall stations located throughout Peninsular Spain were analyzed to determine the IDF curves, and they concluded that the IDF curves of any station can be obtained from the following equation:

$$I(t,p) \approx I(t_0,p_0)\left(\frac{p}{p_0}\right)^{0.24}\left(\frac{t}{t_0}\right)^{n_{med}} \quad (1)$$

where $I(t,p)$ is the maximum mean intensity based on the duration, t, and the return period, p. $I(t_0,p_0)$ is the baseline intensity, the exponent n_{med} is characteristic of the local meteorology, and $I(t,p)$ was estimated for all rainfall stations used in the study.

Therefore, using the equation above and the n_{med} coefficients estimated in Moncho et al. (2009), RAINHHMX was assessed in four stages: (1) Extraction of the maximum daily intensity, $I(24,35)$, from AEMET dataset (1979–2013) for the 64 rainfall stations, and calculation of the maximum half-hour rainfall, $I(0.5,35)$, based on Eq. 1 using R script; (2) Estimation of the torrentiality index as the relation between $I(0.5,35)$ and $I(24,35)$ and spatial representation of this index using ArcGis 10.2; (3) Application of the kriging technique to obtain torrentiality index values at a 5 km resolution (Fig. 2). The kriging method has strong theoretical support (Tabios and Salas, 1985), and according to Li and Heap (2011), it performs better than non-geostatistical methods. Ordinary kriging and hypothetical spherical variogram (Solana-Gutiérrez and Merino-de-Miguel, 2011) options from ArcGIS were used in this study. Finally, (4) RAINHHMX was estimated by using an R script to extract $I(24,35)$ per month throughout Peninsular Spain and multiplying these values by the corresponding torrentiality index.

2.3. Performance evaluation of the WGEN statistics obtained from the PSWG dataset

2.3.1. Study area and data sources

Because of its complex orography and geographical location between the subtropical zone and the European mild zone, Peninsular Spain presents a vast range of climatic variability (Senent-Aparicio et al., 2018b), including some of the most arid European areas in the southeast and the rainiest areas in the north (Pérez-Sánchez et al., 2019). In this study, the basins were selected to consider the main climatic zones found in Peninsular Spain, following the Köppen-Geiger climate grading system (Kottek et al., 2006).

As shown in Fig. 3, Labrada River basin (LRB) is situated at the north of the Miño-Sil Basin (NW Spain) and the weather in this area is a warm-summer Mediterranean (Csb) climate, which is characterized by cool to mild and wet winters and warm and dry summers. Magasca River basin (MRB) is a tributary of the Almonte River and is part of the Tagus River network. The climate in the MRB is a hot-summer Mediterranean (Csa) climate, which is dominant in Peninsular Spain (AEMET, 2011), with monthly mean temperatures ranging from 7.4 °C in January to 25.0 °C in July. Finally, Ega River basin (ERB) falls within a warm temperature humid climate characterized by warm summers (Cfb), with monthly mean temperatures ranging from 3.1 °C in February to 18.5 °C in August. Based on the UNESCO Classification limits of the Aridity Index (Nastos et al., 2013), MRB, LRB and ERB can be classified as semi-arid, humid

Table 3
Parameters used to calibrate the SWAT model. (r_) means relative change, it means that the current parameter must be multiplied by (1 + the value obtained in the calibration), (v_) refers to the substitution of the existing parameter value by the value determined in the calibration, and (a_) means absolute change, it means that the adjusted value must be summed up with the original parameter value.

Parameter	Description	Range	ERB	MRB	LRB
r_CN2.mgt	SCS runoff curve number	–0.2 to 0.2	–0.13	−0.14	−0.0135
v_ALPHA_BF.gw	Baseflow alpha factor (days−1)	0 to 0.7	0.07	0.35	0.09
a_GW_DELAY.gw	Groundwater delay time (days)	–10 to 60	7.11	3.04	2.52
a_GWQMN.gw	Threshold depth of water in the shallow aquifer for return flow to occur (mm)	−200 to 1500	796.50	−10.83	82.50
v_GW_REVAP.gw	Groundwater revap coefficient	0.02 to 0.2	0.04	0.09	–
a_REVAPMN.gw	Threshold depth of water in the shallow aquifer for revap or percolation to the deep aquifer to occur (mm)	–200 to 200	33.65	−165.75	–
v_EPCO.bsn	Plant uptake compensation factor	0.5 to 1	0.84	0.87	–
v_ESCO.bsn	Soil evaporation compensation factor	0.3 to 0.95	0.60	0.47	0.77
r_SOL_AWC.sol	Available water capacity of the soil layer (mm H2O/mm soil)	–0.2 to 0.2	–0.001	0.10	−0.013
v_LAT_TTIME.hru	Lateral flow travel time (day)	0 to 180	38.92	1.40	3.95
v_RCHRG_DP.gw	Deep aquifer percolation fraction	0−1	–	–	0.01
v_CH_K1.rte	Effective hydraulic conductivity for tributary channel (mm h^{-1})	0 to 300	–	–	6.98
v_CH_N2.rte	Manning coefficient for main channel	0.01 to 0.3	–	–	0.13
v_CH_N1.rte	Manning coefficient for tributary channel	0.01 to 0.3	–	–	0.19
r_SOL_K.sol	Soil saturated hydraulic conductivity (mm h^{-1})	−0.2 to 0.2	–	–	0.12
r_SLSUBBSN.hru	Average slope length (m)	−0.2 to 0.2	–	–	−0.006
v_OV_N.hru	Overland Manning roughness	0.01 to 0.80	–	–	0.69

Marco da Curra (43.34°N,7.89°O)

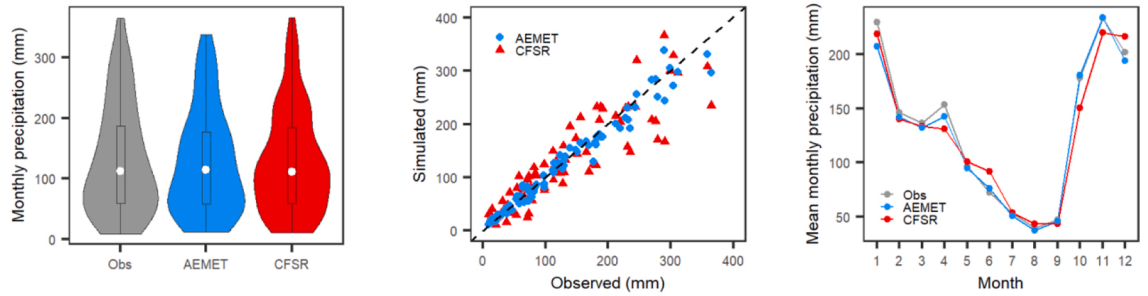

Guitiriz-Mirador (43.22°N,7.78°O)

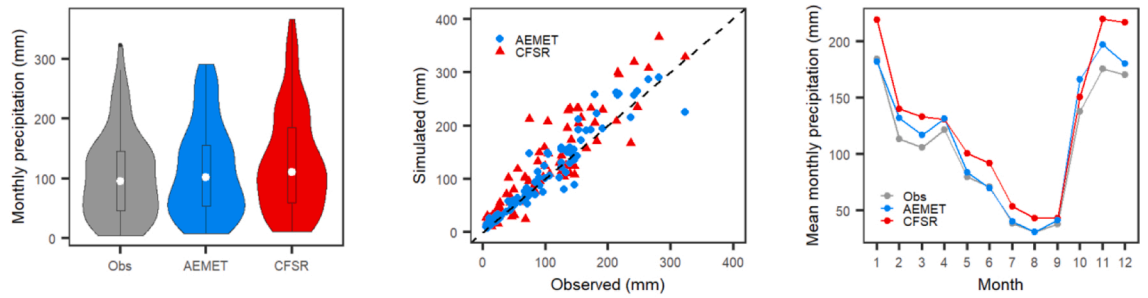

Madroñera (39.46°N,5.76°O)

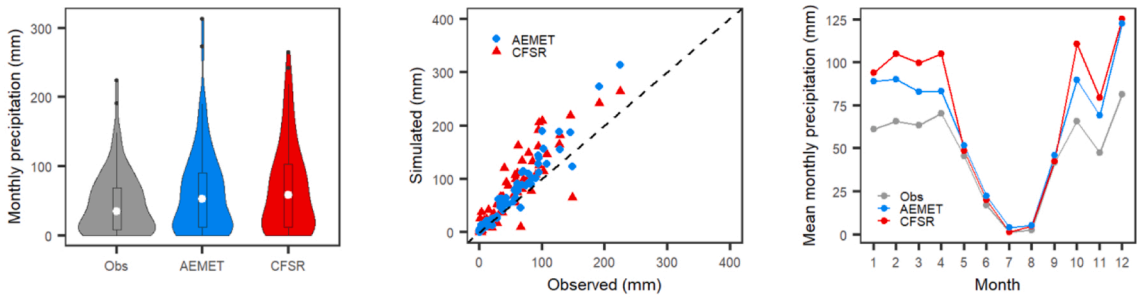

Navarrete (42.64°N,2.52°O)

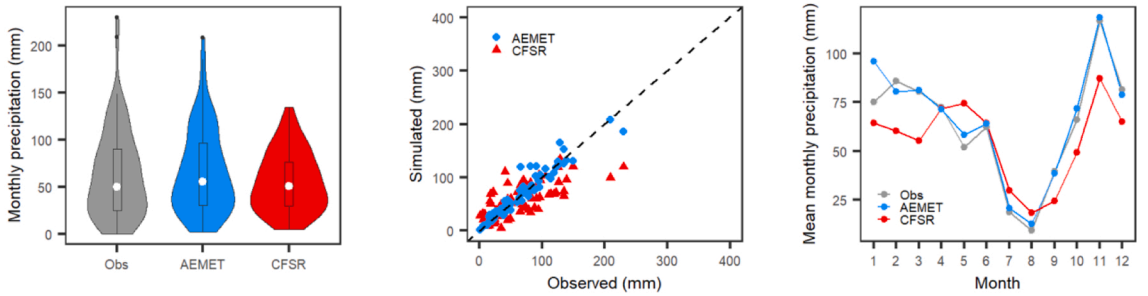

Herrera (42.60°N,2.68°O)

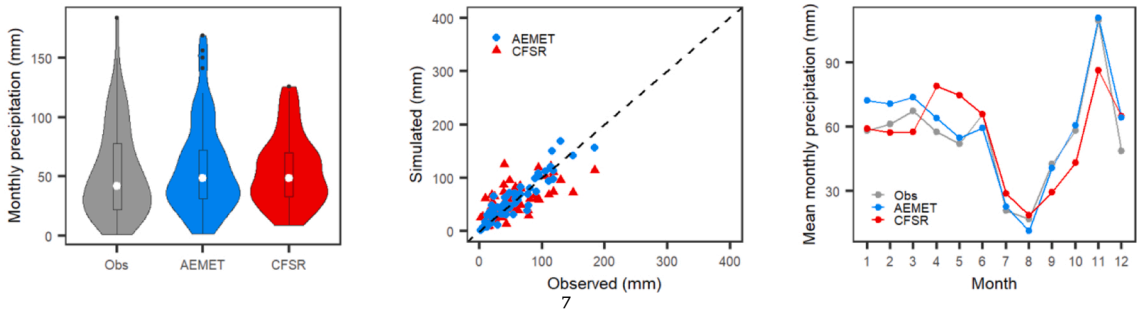

(caption on next page)

Fig. 4. Comparison of average monthly observed precipitation with PSWG and CFSR datasets based on the period 2007-2013 using violin plots (left column), scatterplots (central column) and variations of rainfall patterns (right column).

and sub-humid basins, respectively. Table 2 summarizes the characteristics of the watersheds used for the technical validation of the dataset.

Version 1.8 of the QGIS interface for SWAT, QSWAT (Dile et al., 2016), was used to build the model with freely available information. The input data for the SWAT model in this study include topography, land use, soil and discharge data. The digital elevation model (DEM) at 30 m spatial resolution was obtained from the National Geographic Institute of Spain. Soil data was extracted from the Harmonized World Soil Database (HWSD), developed by the Food and Agriculture Organization of the United Nations (FAO) and containing 16,000 mapping units with two different soil layers (0−300 mm and 300−1,000 mm deep) (Nachtergaele et al., 2010). Land cover maps were derived from Corine Land Cover and surface slope type was classified into three classes (< 2%, 2–8%, > 8%). According to the FAO criteria for preparation of soil degradation maps, slopes below 8% lead to rill and interrill erosion, and when slopes are above 8%, gully erosion takes place (Molina-Navarro et al., 2014). Land cover on the LRB consists of shrublands (34 %), agricultural areas (24 %) and forest (19 %) while the major land cover in the MRB is grassland (25 %) followed by cropland-grassland mosaics (19 %). ERB is a mostly forest-dominated area which covers about 68 % of the basin, and 18 % is covered by agricultural areas. Rainfall and temperature data were obtained for LRB, ERB and MRB from MeteoGalicia (https://www.meteogalicia.gal), Euskalmet (https://www.euskalmet.euskadi.eus), and Redarex (http://redarexplus.gobex.es) websites, respectively. Data on streamflows were available from the website of the Spanish Centre for Hydrographic Studies (CEDEX) (https://ceh.cedex.es/anuarioaforos/default.asp), where data are updated to September 2017.

2.3.2. SWAT model calibration

For dataset evaluation, the time period October 2011 – September 2017 was selected, due to the common availability of streamflow data in the three watersheds. A three-year warm-up period was selected to achieve a steady state for the SWAT model. Using our previous experience in similar watersheds, ten commonly used flow calibration parameters and their ranges were chosen, incorporating aspects of surface runoff, groundwater, and soil data. Automatic monthly calibration was performed in the EGA and MRB by means of the SWAT-CUP software (Abbaspour, 2007) and one of the algorithms which it provides: the Sequential Uncertainty Adjustment (SUFI-2). NSE was used as the objective function and 2000 simulations were run. In the case of LRB, parameter calibration was not necessary, because a previously calibrated model in this basin was used to simulate the initial scenario (Jimeno-Sáez et al., 2018). The list of the adjusted SWAT parameters, showing the range of variation and the final values obtained after the calibration process, is given in Table 3.

2.3.3. Validation approach

After the calibration process, we compared monthly flow simulations in the LRB, MRB and ERB based on different precipitation data availability scenarios. For each of the scenarios, a certain percentage of precipitation data has been eliminated (from 10 to 60 %), and the gaps generated have been filled independently with both the PSWG dataset and the CFSR dataset. The monthly scale has been used for validation, as at daily scale, WGEN can estimate unrealistic daily values, whereas at monthly scale, the generated values are reasonable for water resources planning studies (Bae et al., 2011).

2.3.4. Performance evaluation criteria

We assessed and compared SWAT outputs based on four statistical evaluation criteria, including the Nash Sutcliffe efficiency coefficient (NSE), percent bias (PBIAS), the standard deviation ratio of observed data (RSR), and Kling Gupta efficiency coefficient (KGE), which are the most commonly applied in hydrological research (Jimeno-Sáez et al., 2018). According to Moriasi et al. (2007), the model performance is considered satisfactory when the PBIAS is in the range of ±25 %, NSE is above 0.5, and RSR is below 0.7. A

Table 4
Daily statistical indices.

Station	Precipitation dataset	CC	RMSE (mm)	ME (mm)	BIAS (%)	POD	FAR	CSI	PD1	PD10
	Local	–	–	–	–	–	–	–	853	327
Marco da Curra	AEMET	0.92	3.37	−0.11	−2.54	0.96	0.18	0.80	1029	325
	CFSR	0.80	5.10	−0.07	−1.76	0.91	0.20	0.74	1010	294
	Local	–	–	–	–	–	–	–	789	268
Guitiriz-Mirador	AEMET	0.86	3.66	0.28	8.37	0.94	0.22	0.75	958	279
	CFSR	0.80	4.84	0.75	22.11	0.93	0.26	0.70	1010	294
	Local	–	–	–	–	–	–	–	400	114
Madroñera	AEMET	0.83	2.80	0.29	18.62	0.86	0.27	0.65	480	135
	CFSR	0.76	3.78	0.63	40.75	0.89	0.31	0.64	530	156
	Local	–	–	–	–	–	–	–	575	129
Navarrete	AEMET	0.78	3.36	0.09	4.39	0.86	0.27	0.65	688	138
	CFSR	0.63	4.16	−0.23	−11.12	0.78	0.40	0.51	763	75
	Local	–	–	–	–	–	–	–	540	99
Herrera	AEMET	0.71	3.31	0.20	10.93	0.78	0.31	0.58	623	101
	CFSR	0.56	3.73	0.11	5.98	0.77	0.39	0.51	710	74

Marco da Curra (43.34°N,7.89°O)

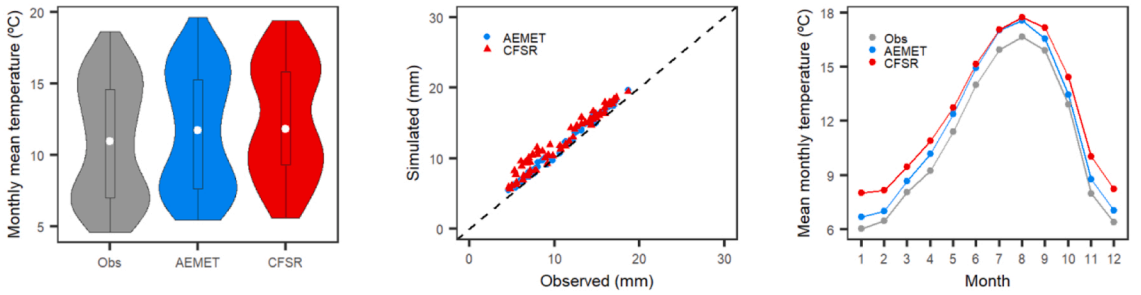

Guitiriz-Mirador (43.22°N,7.78°O)

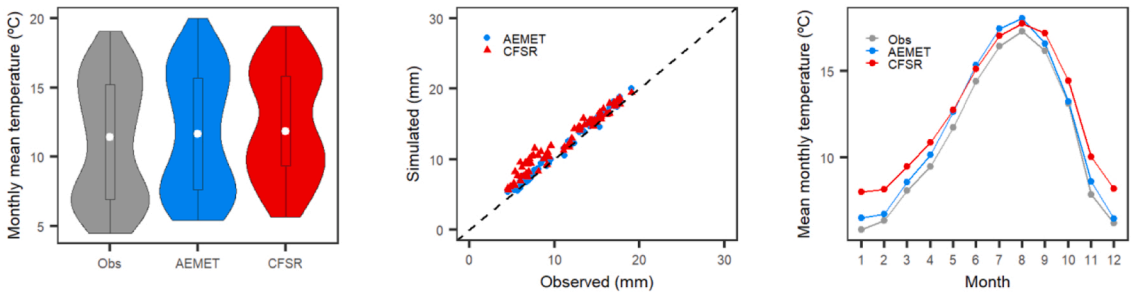

Madroñera (39.46°N,5.76°O)

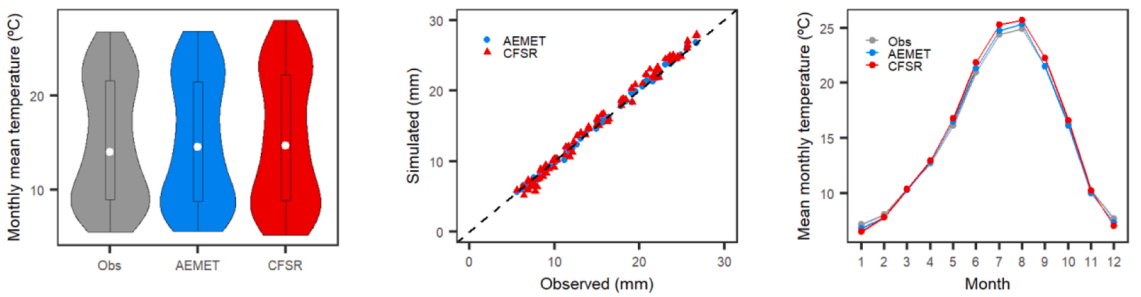

Navarrete (42.64°N,2.52°O)

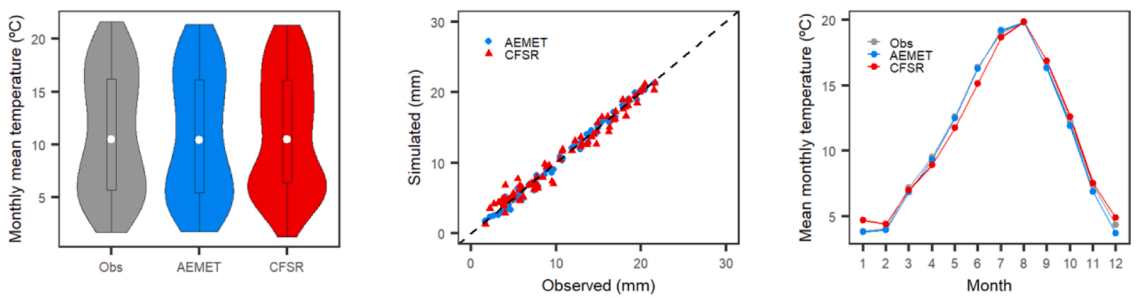

Herrera (42.60°N,2.68°O)

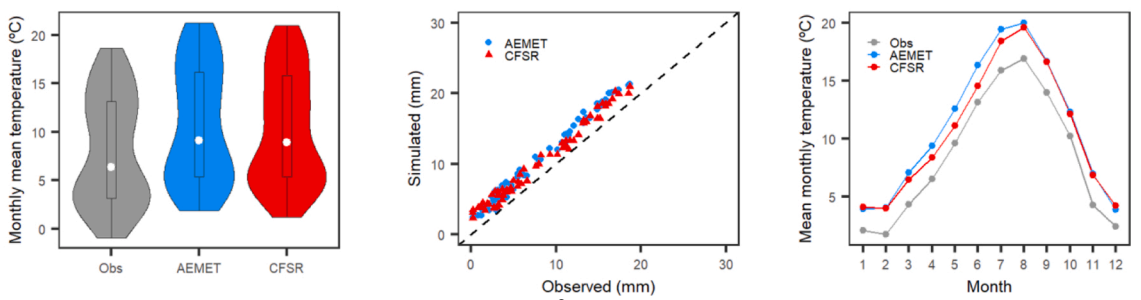

(caption on next page)

Fig. 5. Comparison of average monthly observed temperature with PSWG and CFSR datasets based on the period 2007-2013 using violin plots (left column), scatterplots (central column) and variations of temperature patterns (right column).

KGE performance above 0.5 is considered satisfactory (Brighenti et al., 2019).

3. Results and discussion

3.1. Precipitation comparison

Prior to the analysis of the performance of the statistics generated by PSWG and CFSR in the simulation of flows, the observed data have been compared on a monthly scale with the data derived from PSWG and CFSR. The aim of this comparison is to evaluate the quality of the datasets against the historical rainfall data observed in the 5 rainfall stations where the data were used (Marco da Curra and Guitiriz-Mirador in LRB; Madroñera and Navarrete in ERB; Herrera in MRB), allowing a better understanding of the deviations related to the flow simulation. The monthly distribution and seasonality have been analyzed (Fig. 4) for the common time period (2007–2013) when rainfall data was available from all data sources (observed, PSWG and CFSR). Firstly, we have used violin plots to simultaneously visualize data distribution and probability density combining boxplots with a kernel density diagram. No significant differences are detected in the prediction of the median (white point in graphs), while the shape of the density distribution has a clearly more accurate fit using the AEMET data, especially if we examine the Navarrete and Herrera stations. Overall, the violin plots indicated superior model performance for the AEMET data, which fitted closely with the observations, in contrast to the CFSR data. Moreover, the scatterplots of the AEMET and CFSR monthly rainfall versus observed data are also presented. The scatterplots indicate that the AEMET data seems to fit better on all stations. This fact is confirmed from the values of the coefficient of determination (R^2) obtained. Based on AEMET data, R^2 values in Marco da Curra, Guitiriz, Madroñera, Navarrete y Herrera rainfall stations were 0.97, 0.89, 0.94, 0.92 and 0.85, respectively, while using CFSR dataset, R^2 values were 0.81, 0.81, 0.80, 0.52 and 0.44, respectively. Finally, mean monthly rainfall pattern was analyzed at the same stations. The monthly rainfall patterns are similar, being July and August the driest months, and concentrating the rainfall between the months of November and January. Similar to the conclusions obtained through the violin and scatter plots, AEMET's rainfall estimates are closer to the observed data. For example, it can be noted that in Navarrete station the rainfall is underestimated by CFSR during the rainiest months, while in Guitiriz or Madroñera it is overestimated. Similar conclusions were obtained in the work published by Senent-Aparicio et al. (2018b) where precipitation data from AEMET's 5 km grid was compared with additional gridded datasets (CFSR, TRMM, MSWEP and PERSIANN) over Peninsular Spain.

The ability to detect daily precipitation events was also assessed by estimating three categorical statistics. The probability of detection (POD), which represents the ratio of rainy days that were correctly predicted. A perfect POD estimation is equal to 1. The false alarm ratio (FAR), which measures precipitation detections that did not actually occur, i.e. precipitation that was detected by the precipitation product but not by the rain gauges. The value of this ratio varies between 0 and 1, being 0 the optimal value. The critical success index (CSI) considers both situations and is based on POD and FAR, being 1 the optimal value. To measure the accuracy of the rainfall datasets in terms of precipitation amount and timing patterns, six additional indicators were employed: 1) correlation coefficient (CC); 2) root mean square error (RMSE); 3) mean error (ME); 4) relative bias (BIAS); 5) total number of days in which rainfall exceeds 1 (PD1) or 6) 10 mm (PD10). The results, shown in Table 4, indicates that AEMET was in better agreement with local stations, with high precipitation detection ability, compared with the CFSR dataset. As can be drawn from the indicators related to the number of rainy days, both AEMET and CFSR tend to overestimate the number of rainy days. However, AEMET performs better than CFSR in terms of the number of days with heavy rainfall events (10 mm threshold).

3.2. Temperature comparison

Similarly to the previous section, the observed temperature have been also compared on a monthly scale with the data derived from PSWG and CFSR (Fig. 5). Similar performances are observed at the Marco da Curra and Guitiriz-Mirador stations. Both AEMET and CFSR overestimate temperatures in the summer months, while in the winter months, AEMET temperatures are more in accordance with observed temperatures. At the station located in the MRB, Madroñera, both datasets fit the observed values adequately. However, the shape of the density distribution presents a more accurate fit using the AEMET data. Finally, the two weather stations used in ERB show different trends. On the one hand, the Navarrete station shows a good fit regardless of the data set used. On the other hand, at the Herrera station, both AEMET and CFSR overestimate the temperature values, which can be explained by the location of the station in a high mountain area with steep slopes in the surroundings.

3.3. PSWG performance evaluation

In this section, performance of the PSWG and CFSR datasets was compared using six different scenarios, where missing rates from 10 to 60 % were applied and missing data were filled in using both datasets. Finally, we compared SWAT model outputs from these scenarios with model results using complete historical data. As shown in Table 4, the PSWG dataset clearly outperforms CFSR, especially when missing rates exceed 50 %. When the missing rate was gradually increased, NSE, PBIAS, RSR and KGE exhibited the same worsening trends. In wetter climate basins, model results for even higher missing rates (60 %) are acceptable, with NSE values

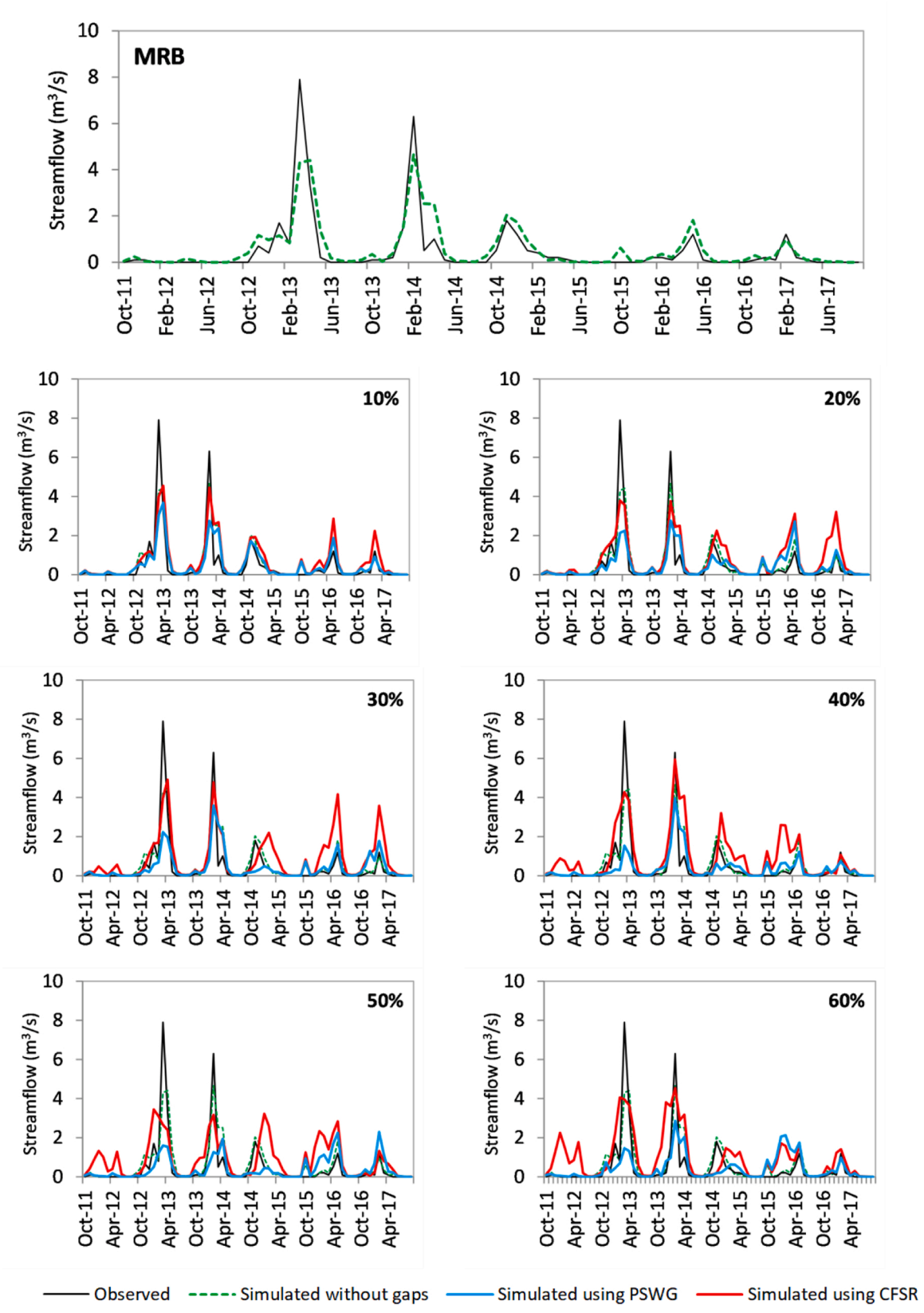

Fig. 6. Streamflow variability using different datasets in the MRB.

Table 5
Evaluation of the simulation results for the different temporal data scarcities.

Basin	Missing Rate	NSE		PBIAS		RSR		KGE	
		PSWG	CFSR	PSWG	CFSR	PSWG	CFSR	PSWG	CFSR
MRB	0%	0.75		−22.65		0.50		0.67	
	10%	0.60	0.66	−0.66	−40.62	0.63	0.58	0.56	0.52
	20%	0.48	0.48	3.19	−63.53	0.72	0.72	0.45	0.29
	30 %	0.50	0.39	10.78	−82.06	0.71	0.78	0.47	0.13
	40%	0.44	0.33	19.77	−95.80	0.75	0.82	0.39	0.01
	50 %	0.26	0.15	16.87	−85.05	0.86	0.92	0.25	0.02
	60 %	0.31	0.17	6.16	−103.7	0.83	0.91	0.33	−0.10
LRB	0%	0.88		−12.84		0.35		0.78	
	10%	0.89	0.90	−6.95	−12.59	0.33	0.32	0.86	0.83
	20%	0.89	0.85	−2.49	−15.26	0.33	0.39	0.92	0.82
	30 %	0.86	0.84	−2.81	−12.65	0.37	0.40	0.90	0.85
	40%	0.80	0.79	−1.28	−15.98	0.44	0.46	0.89	0.80
	50 %	0.78	0.69	3.10	−13.26	0.47	0.55	0.82	0.79
	60 %	0.72	0.57	5.93	−12.55	0.53	0.66	0.77	0.74
ERB	0%	0.76		8.11		0.48		0.79	
	10%	0.79	0.76	10.94	10.16	0.45	0.48	0.80	0.79
	20%	0.75	0.79	13.36	6.04	0.49	0.45	0.74	0.82
	30 %	0.70	0.70	12.60	13.85	0.55	0.55	0.70	0.69
	40%	0.68	0.69	22.19	14.68	0.54	0.55	0.61	0.65
	50 %	0.65	0.65	19.87	19.07	0.59	0.58	0.59	0.60
	60 %	0.61	0.60	23.17	23.80	0.61	0.62	0.65	0.65

above 0.5, PBIAS below 25, and RSR below 0.70. In the case of ERB, the results obtained with the PSWG and CFSR datasets are very similar. However, in the case of LRB, the results obtained with PSWG are higher than those of CFSR, and this difference becomes more pronounced as the missing rate increases. In the case of the MRB, which is characterized by its semi-arid climate, the relative superiority of the PSWG dataset is also evident here. However, model performance worsens significantly as the missing rates increase, and the PSWG dataset results are not acceptable for missing rates above 30 %. These results can be explained by the pluviometric regime characteristic of semi-arid Mediterranean climates, which are characterized by episodes of heavy rainfall, characterized by short and very intense rainfall, which cause large floods with a markedly torrential character (Senent-Aparicio et al., 2016). Pérez-Sánchez et al. (2019) indicated, based on the application of six hydrological models in sixteen different basins over Peninsular Spain, that the climatic characteristics of the watershed are the most important factor in a hydrological model's performance. In addition, the effectiveness of the CFSR dataset in this watershed is much lower than that of the PSWG dataset.

In MRB, CFSR data significantly increases the simulated water volume as the missing rate increases (Fig. 6), resulting in increasing PBIAS that can double simulated water volumes, compared with observed ones, for scenarios with a higher missing rate (60 %). These results were expected based on previous findings that indicated a global trend in CFSR data to generally overestimate both rainfall and the number of rainy days (Dhanesh et al., 2020). In case studies where the initial PBIAS is positive, and therefore the total volume generated is underestimated, the CFSR dataset allows for acceptable data generation. However, in such basins as MRB, where the initial PBIAS is -22.65 %, use of the CFSR dataset causes an important worsening of the model performance (Table 5).

4. Conclusions

Meteorological data are the main drivers of hydrological modelling. However, available meteorological data can have gaps in the data series and often have limited spatial coverage for use in hydrological models such as the SWAT model. To address this limitation, SWAT includes a weather data generator algorithm that can complete these data based on long-term weather statistics. This work presents a set of weather statistics data (PSWG) calculated for the whole Peninsular Spain that provides a higher resolution than the statistics calculated from CFSR available on the SWAT website. PSWG dataset has been tested in three different basins under the most representative climatic conditions of the Peninsular Spain showing an improvement in the monthly flow simulation.

A clear limitation of this work is that daily data on relative humidity, solar radiation and wind speed from CFSR are available until July 2014, so the statistics have been calculated for the common period (1979–2013). However, the satellite datasets continue to improve, so the authors encourage the need for further studies using different satellite data products, as well as the use of a larger number of test basins for verification considering the climatic diversity that characterizes Peninsular Spain.

To ensure a broader impact from this work's results, all weather datasets generated in this study were made available online to promote other SWAT modelling approaches in peninsular Spain. As stated in Abbaspour et al. (2019), data preparation is extremely time-consuming and susceptible to errors, resulting in much of the research time being spent on data processing instead of output analysis. The PSWG dataset is archived for long-term storage on the SWAT model website (https://swat.tamu.edu/data/) and consists of two WGEN database files in Microsoft Access and SQLite file format that can be used in SWAT and SWAT+, respectively. SWAT + is a renovated version of the SWAT model, aimed at solving previous weaknesses and improving the spatial representation of processes' interactions (Bieger et al., 2017), that uses the SQLite database engine for data storage. Besides, AEMET gridded precipitation and temperature data are available in ready-to-use SWAT format at the same url.

CRediT authorship contribution statement

Javier Senent-Aparicio: Conceptualization, Methodology, Writing - original draft. **Patricia Jimeno-Sáez:** Formal analysis, Validation. **Adrián López-Ballesteros:** Formal analysis, Validation. **José Ginés Giménez:** Data curation, Software. **Julio Pérez-Sánchez:** Validation, Writing - review & editing. **José M. Cecilia:** Funding acquisition, Software, Writing - review & editing. **Raghavan Srinivasan:** Supervision, Writing - review & editing.

Declaration of Competing Interest

The authors declare that they have no known competing financial interests or personal relationships that could have appeared to influence the work reported in this paper.

Acknowledgements

This research was funded by the Ministry of Science, Innovation and Universities of Spain under grants RTC-2017-6389-5 and RTI2018-096384-B-I00. This work has also received funding from the European Union's Horizon 2020 research and innovation programme within the framework of the project SMARTLAGOON under grant agreement No. 101017861. Adrián López Ballesteros was sponsored by the Ministry of Science, Innovation and Universities of Spain under an FPU grant (FPU17/00923) and José M. Cecilia under the Ramon y Cajal Program (Grant No. RYC2018-025580-I). The authors would like to acknowledge AEMET for the precipitation and air temperature data provided for this work (AEMET grid dataset can be found at http://www.aemet.es/es/serviciosclimaticos/cambio_climat).

Appendix A. Supplementary data

Supplementary material related to this article can be found, in the online version, at doi:https://doi.org/10.1016/j.ejrh.2021.100826.

References

Abbaspour, K.C., 2007. User Manual for SWAT-CUP. SWAT Calibration and Uncertainty Analysis Programs. Swiss Federal Institute of Aquatic Science and Technology, Eawag, Duebendorf, Switzerland.

Abbaspour, K.C., Vaghefi, S.A., Yang, H., Srinivasan, R., 2019. Global soil, landuse, evapotranspiration, historical and future weather databases for SWAT Applications. Sci. Data 6, 263. https://doi.org/10.1038/s41597-019-0282-4.

AEMET, 2011. Iberian Climate Atlas. AEMET. Ministerio de Medio Ambiente y Rural y Marino, Madrid, Spain.

AEMET [WWW Document], 2020. URL http://www.aemet.es/en/serviciosclimaticos (accessed 8.6.20).

Alodah, A., Seidou, O., 2019. The adequacy of stochastically generated climate time series for water resources systems risk and performance assessment. Stoch. Environ. Res. Risk Assess. 33, 253–269. https://doi.org/10.1007/s00477-018-1613-2.

Amblar-Francés, M.P., Ramos-Calzado, P., Sanchis-Lladó, J., Hernanz-Lázaro, A., Peral-García, M.C., Navascués, B., Dominguez-Alonso, M., Pastor-Saavedra, M.A., Rodríguez-Camino, E., 2020. High Resolution Climate Change Projections for the Pyrenees Region, p. 18.

Arnold, J.G., Srinivasan, R., Muttiah, R.S., Williams, J.R., 1998. Large area hydrologic modeling and assessment part I: model Development. J. Am. Water Resour. Assoc. 34, 73–89. https://doi.org/10.1111/j.1752-1688.1998.tb05961.x.

Arnold, J.G., Kiniry, J.R., Srinivasan, R., Williams, J.R., Haney, E.B., Neitsch, S.L., 2012. SWAT 2012 Input/Output Documentation.

Bae, D.-H., Jung, I.-W., Lettenmaier, D.P., 2011. Hydrologic uncertainties in climate change from IPCC AR4 GCM simulations of the Chungju Basin, Korea. J. Hydrol. 401, 90–105. https://doi.org/10.1016/j.jhydrol.2011.02.012.

Baena-Ruiz, L., Pulido-Velazquez, D., Collados-Lara, A.-J., Renau-Pruñonosa, A., Morell, I., Senent-Aparicio, J., Llopis-Albert, C., 2020. Summarizing the impacts of future potential global change scenarios on seawater intrusion at the aquifer scale. Environ. Earth Sci. 79, 99. https://doi.org/10.1007/s12665-020-8847-2.

Bieger, K., Arnold, J.G., Rathjens, H., White, M.J., Bosch, D.D., Allen, P.M., Volk, M., Srinivasan, R., 2017. Introduction to SWAT+, a completely restructured version of the soil and water assessment tool. JAWRA J. Am. Water Resour. Assoc. 53, 115–130. https://doi.org/10.1111/1752-1688.12482.

Brighenti, T.M., Bonumá, N.B., Grison, F., Mota, A., de, A., Kobiyama, M., Chaffe, P.L.B., 2019. Two calibration methods for modeling streamflow and suspended sediment with the swat model. Ecol. Eng. 127, 103–113. https://doi.org/10.1016/j.ecoleng.2018.11.007.

Cánovas, C.R., Macías, F., Olías, M., 2018. Hydrogeochemical behavior of an anthropogenic mine aquifer: implications for potential remediation measures. Sci. Total Environ. 636, 85–93. https://doi.org/10.1016/j.scitotenv.2018.04.270.

Chen, J., Brissette, F., Zhang, X.J., 2014. Multi-site stochastic weather generator for daily precipitation and temperature. Trans. ASABE 1375–1391. https://doi.org/10.13031/trans.57.10685.

Chen, J., Arsenault, R., Brissette, F.P., Côté, P., Su, T., 2019. Coupling annual, monthly and daily weather generators to simulate multisite and multivariate climate variables with low-frequency variability for hydrological modelling. Clim. Dyn. 53, 3841–3860. https://doi.org/10.1007/s00382-019-04750-z.

Dai, C., Qin, X.S., 2019. Assessment of the effectiveness of a multi-site stochastic weather generator on hydrological modelling in the Red Deer River watershed. Canada. Hydrol. Sci. J. 64, 1616–1628. https://doi.org/10.1080/02626667.2019.1661416.

Dhanesh, Y., Bindhu, V.M., Senent-Aparicio, J., Brighenti, T.M., Ayana, E., Smitha, P.S., Fei, C., Srinivasan, R., 2020. A comparative evaluation of the performance of CHIRPS and CFSR data for different climate zones using the SWAT model. Remote Sens. (Basel) 12, 3088. https://doi.org/10.3390/rs12183088.

Dile, Y.T., Daggupati, P., George, C., Srinivasan, R., Arnold, J., 2016. Introducing a new open source GIS user interface for the SWAT model. Environ. Model. Softw. 85, 129–138. https://doi.org/10.1016/j.envsoft.2016.08.004.

Duan, Z., Tuo, Y., Liu, J., Gao, H., Song, X., Zhang, Z., Yang, L., Mekonnen, D.F., 2019. Hydrological evaluation of open-access precipitation and air temperature datasets using SWAT in a poorly gauged basin in Ethiopia. J. Hydrol. (Amst) 569, 612–626. https://doi.org/10.1016/j.jhydrol.2018.12.026.

Essenfelder, A.H., 2018. SWAT Weather Database: A Quick Guide.

Essenfelder, A.H., Pérez-Blanco, C.D., Mayer, A.S., 2018. Rationalizing systems analysis for the evaluation of adaptation strategies in complex human-water systems. Earths Future 6, 1181–1206. https://doi.org/10.1029/2018EF000826.

Gao, X., Zhu, Q., Yang, Z., Wang, H., 2018. Evaluation and hydrological application of CMADS against TRMM 3B42V7, PERSIANN-CDR, NCEP-CFSR, and gauge-based datasets in Xiang River Basin of China. Water 10, 1225. https://doi.org/10.3390/w10091225.

Ghimire, U., Akhtar, T., Shrestha, N., Daggupati, P., 2019. Development of Asia Pacific Weather Statistics (APWS) dataset for use in Soil and Water Assessment Tool (SWAT) simulation (preprint). Hydrology and Soil Science – Hydrology. https://doi.org/10.5194/essd-2019-178.

Herrera, S., Fernández, J., Gutiérrez, J.M., 2016. Update of the Spain02 gridded observational dataset for EURO-CORDEX evaluation: assessing the effect of the interpolation methodology: EURO-CORDEX COMPLIANT UPDATE OF SPAIN02. Int. J. Climatol. 36, 900–908. https://doi.org/10.1002/joc.4391.

Jimeno-Sáez, P., Senent-Aparicio, J., Pérez-Sánchez, J., Pulido-Velazquez, D., 2018. A comparison of SWAT and ANN models for daily runoff simulation in different climatic zones of Peninsular Spain. Water 10, 192. https://doi.org/10.3390/w10020192.

Jodar-Abellan, A., Valdes-Abellan, J., Pla, C., Gomariz-Castillo, F., 2019. Impact of land use changes on flash flood prediction using a sub-daily SWAT model in five Mediterranean ungauged watersheds (SE Spain). Sci. Total Environ. 657, 1578–1591. https://doi.org/10.1016/j.scitotenv.2018.12.034.

Kottek, M., Grieser, J., Beck, C., Rudolf, B., Rubel, F., 2006. World Map of the Köppen-Geiger climate classification updated. Meteorol. Z. 15, 259–263. https://doi.org/10.1127/0941-2948/2006/0130.

Li, J., Heap, A.D., 2011. A review of comparative studies of spatial interpolation methods in environmental sciences: performance and impact factors. Ecol. Inform. 6, 228–241. https://doi.org/10.1016/j.ecoinf.2010.12.003.

López-Ballesteros, A., Senent-Aparicio, J., Srinivasan, R., Pérez-Sánchez, J., 2019. Assessing the Impact of Best Management Practices in a Highly Anthropogenic and Ungauged Watershed Using the SWAT Model: A Case Study in the El Beal Watershed (Southeast Spain). Agronomy 9, 576. https://doi.org/10.3390/agronomy9100576.

Malik, W., Jiménez-Aguirre, M.-T., Dechmi, F., 2020. Coupled DSSAT-SWAT models to reduce off-site N pollution in Mediterranean irrigated watershed. Sci. Total Environ. 745, 141000 https://doi.org/10.1016/j.scitotenv.2020.141000.

Meaurio, M., Zabaleta, A., Boithias, L., Epelde, A.M., Sauvage, S., Sánchez-Pérez, J.-M., Srinivasan, R., Antiguedad, I., 2017. Assessing the hydrological response from an ensemble of CMIP5 climate projections in the transition zone of the Atlantic region (Bay of Biscay). J. Hydrol. (Amst) 548, 46–62. https://doi.org/10.1016/j.jhydrol.2017.02.029.

Meng, X., Zhang, X., Yang, M., Wang, H., Chen, J., Pan, Z., Wu, Y., 2019. Application and Evaluation of the China Meteorological Assimilation Driving Datasets for the SWAT Model (CMADS) in Poorly Gauged Regions in Western China. Water 11, 2171. https://doi.org/10.3390/w11102171.

Molina-Navarro, E., Martínez-Pérez, S., Sastre-Merlín, A., Bienes-Allas, R., 2014. Hydrologic modeling in a small Mediterranean Basin as a tool to assess the feasibility of a limno-reservoir. J. Environ. Qual. 43, 121–131. https://doi.org/10.2134/jeq2011.0360.

Moncho, R., Belda, F., Caselles, V., 2009. Climatic study of the exponent "n" in IDF curves: application for the Iberian Peninsula. Tethys 6, 3–14. https://doi.org/10.3369/tethys.2009.6.01.

Moriasi, D.N., Arnold, J.G., Liew, M.W.V., Bingner, R.L., Harmel, R.D., Veith, T.L., 2007. Model evaluation guidelines for systematic quantification of accuracy in watershed simulations. Trans. ASABE 50, 885–900. https://doi.org/10.13031/2013.23153.

Nastos, P.T., Politi, N., Kapsomenakis, J., 2013. Spatial and temporal variability of the aridity index in Greece. Atmospheric Res. 119, 140–152. https://doi.org/10.1016/j.atmosres.2011.06.017.

Neitsch, S.L., Arnold, J.G., Kiniry, J.R., Williams, J.R., 2011. SWAT Theoretical Documentation.

Peral-García, C., Navascués Fernández-Victorio, B., Ramos Calzado, P., 2017. Serie De Precipitación Diaria En Rejilla Con Fines Climáticos.

Peraza-Castro, M., Ruiz-Romera, E., Meaurio, M., Sauvage, S., Sánchez-Pérez, J.M., 2018. Modelling the impact of climate and land cover change on hydrology and water quality in a forest watershed in the Basque Country (Northern Spain). Ecol. Eng. 122, 315–326. https://doi.org/10.1016/j.ecoleng.2018.07.016.

Pérez-Sánchez, J., Senent-Aparicio, J., Segura-Méndez, F., Pulido-Velazquez, D., Srinivasan, R., 2019. Evaluating hydrological models for deriving water resources in Peninsular Spain. Sustainability 11, 2872. https://doi.org/10.3390/su11102872.

Pérez-Sánchez, J., Senent-Aparicio, J., Martínez Santa-María, C., López-Ballesteros, A., 2020. Assessment of ecological and hydro-geomorphological alterations under climate change using SWAT and IAHRIS in the Eo River in Northern Spain. Water 12, 1745. https://doi.org/10.3390/w12061745.

PostgreSQL [WWW Document], 2020. URL https://www.postgresql.org/ (accessed 6.21.20).

Pulido-Velazquez, D., Collados-Lara, A.-J., Alcalá, F.J., 2018a. Assessing impacts of future potential climate change scenarios on aquifer recharge in continental Spain. J. Hydrol. (Amst) 567, 803–819. https://doi.org/10.1016/j.jhydrol.2017.10.077.

Pulido-Velazquez, D., Renau-Pruñonosa, A., Llopis-Albert, C., Morell, I., Collados-Lara, A.-J., Senent-Aparicio, J., Baena-Ruiz, L., 2018b. Integrated assessment of future potential global change scenarios and their hydrological impacts in coastal aquifers – a new tool to analyse management alternatives in the Plana Oropesa-Torreblanca aquifer. Hydrol. Earth Syst. Sci. Discuss. 22, 3053–3074. https://doi.org/10.5194/hess-22-3053-2018.

Richardson, C.W., 1981. Stochastic simulation of daily precipitation, temperature, and solar radiation. Water Resour. Res. 17, 182–190. https://doi.org/10.1029/WR017i001p00182.

Rivas-Tabares, D., Tarquis, A.M., Willaarts, B., De Miguel, Á., 2019. An accurate evaluation of water availability in sub-arid Mediterranean watersheds through SWAT: cega-Eresma-Adaja. Agric. Water Manag. 212, 211–225. https://doi.org/10.1016/j.agwat.2018.09.012.

Roth, V., Lemann, T., 2016. Comparing CFSR and conventional weather data for discharge and soil loss modelling with SWAT in small catchments in the Ethiopian Highlands. Hydrol. Earth Syst. Sci. Discuss. 20, 921–934. https://doi.org/10.5194/hess-20-921-2016.

Rupérez-Moreno, C., Pérez-Sánchez, J., Senent-Aparicio, J., Flores-Asenjo, P., Paz-Aparicio, C., 2017. Cost-Benefit Analysis of the Managed Aquifer Recharge System for Irrigation under Climate Change Conditions in Southern Spain. Water 9, 343. https://doi.org/10.3390/w9050343.

Saha, S., Moorthi, S., Pan, H.-L., Wu, X., Wang, Jiande, Nadiga, S., Tripp, P., Kistler, R., Woollen, J., Behringer, D., Liu, H., Stokes, D., Grumbine, R., Gayno, G., Wang, Jun, Hou, Y.-T., Chuang, H., Juang, H.-M.H., Sela, J., Iredell, M., Treadon, R., Kleist, D., Van Delst, P., Keyser, D., Derber, J., Ek, M., Meng, J., Wei, H., Yang, R., Lord, S., van den Dool, H., Kumar, A., Wang, W., Long, C., Chelliah, M., Xue, Y., Huang, B., Schemm, J.-K., Ebisuzaki, W., Lin, R., Xie, P., Chen, M., Zhou, S., Higgins, W., Zou, C.-Z., Liu, Q., Chen, Y., Han, Y., Cucurull, L., Reynolds, R.W., Rutledge, G., Goldberg, M., 2010. The NCEP climate forecast system reanalysis. Bull. Am. Meteorol. Soc. 91, 1015–1058. https://doi.org/10.1175/2010BAMS3001.1.

Salmoral, G., Willaarts, B.A., Garrido, A., Guse, B., 2017. Fostering integrated land and water management approaches: evaluating the water footprint of a Mediterranean basin under different agricultural land use scenarios. Land Use Policy 61, 24–39. https://doi.org/10.1016/j.landusepol.2016.09.027.

Schuol, J., Abbaspour, K.C., 2007. Using monthly weather statistics to generate daily data in a SWAT model application to West Africa. Ecol. Model. 201, 301–311. https://doi.org/10.1016/j.ecolmodel.2006.09.028.

Senent-Aparicio, J., Pérez-Sánchez, J., Bielsa-Artero, A.M., 2016. Assessment of sustainability in Semiarid Mediterranean Basin: case study of the segura basin. Spain. Tecnol. Cienc. Agua 7, 67–84.

Senent-Aparicio, J., Pérez-Sánchez, J., Carrillo-García, J., Soto, J., 2017. Using SWAT and fuzzy TOPSIS to assess the impact of climate change in the headwaters of the Segura River Basin (SE Spain). Water 9, 149. https://doi.org/10.3390/w9020149.

Senent-Aparicio, J., Liu, S., Pérez-Sánchez, J., López-Ballesteros, A., Jimeno-Sáez, P., 2018a. Assessing impacts of climate variability and reforestation activities on water resources in the headwaters of the Segura River Basin (SE Spain). Sustainability 10, 3277. https://doi.org/10.3390/su10093277.

Senent-Aparicio, J., López-Ballesteros, A., Pérez-Sánchez, J., Segura-Méndez, F., Pulido-Velazquez, D., 2018b. Using multiple monthly water balance models to evaluate gridded precipitation products over Peninsular Spain. Remote Sens. (Basel) 10, 922. https://doi.org/10.3390/rs10060922.

Senent-Aparicio, J., Jimeno-Sáez, P., Bueno-Crespo, A., Pérez-Sánchez, J., Pulido-Velázquez, D., 2019. Coupling machine-learning techniques with SWAT model for instantaneous peak flow prediction. Biosyst. Eng. 177, 67–77. https://doi.org/10.1016/j.biosystemseng.2018.04.022.

Senent-Aparicio, J., Alcalá, F.J., Liu, S., Jimeno-Sáez, P., 2020. Coupling SWAT model and CMB method for modeling of high-permeability bedrock basins receiving interbasin groundwater flow. Water 12, 657. https://doi.org/10.3390/w12030657.

Sharpley, A.N., Williams, J.R., 1990. EPIC - Erosion/Proctivity Impact Calculator.

Solana-Gutiérrez, J., Merino-de-Miguel, S., 2011. A variogram model comparison for predicting forest changes. Procedia Environ. Sci. 7, 383–388. https://doi.org/10.1016/j.proenv.2011.07.066.

SWAT [WWW Document], 2020. SWAT. URL https://swat.tamu.edu/data/ (accessed 8.4.20).

Tabios, G.Q., Salas, J.D., 1985. A COMPARATIVE ANALYSIS OF TECHNIQUES FOR SPATIAL INTERPOLATION OF PRECIPITATION. J. Am. Water Resour. Assoc. 21, 365–380. https://doi.org/10.1111/j.1752-1688.1985.tb00147.x.

Tan, M.L., Gassman, P.W., Cracknell, A.P., 2017. Assessment of three long-term gridded climate products for hydro-climatic simulations in tropical river basins. Water 9, 229. https://doi.org/10.3390/w9030229.

Tan, M.L., Gassman, P.W., Yang, X., Haywood, J., 2020. A review of SWAT applications, performance and future needs for simulation of hydro-climatic extremes. Adv. Water Resour. 143, 103662 https://doi.org/10.1016/j.advwatres.2020.103662.

Thom, V.T., Khoi, D.N., Linh, D.Q., 2017. Using gridded rainfall products in simulating streamflow in a tropical catchment – a case study of the Srepok River Catchment. Vietnam. J. Hydrol. Hydromech. 65, 18–25. https://doi.org/10.1515/johh-2016-0047.

van der Walt, S., Colbert, S.C., Varoquaux, G., 2011. The NumPy array: a structure for efficient numerical computation. Comput. Sci. Eng. 13, 22–30. https://doi.org/10.1109/MCSE.2011.37.

Vesely, F.M., Paleari, L., Movedi, E., Bellocchi, G., Confalonieri, R., 2019. Quantifying uncertainty due to stochastic weather generators in climate change impact studies. Sci. Rep. 9, 9258. https://doi.org/10.1038/s41598-019-45745-4.

White, M., Gambone, M., Haney, E., Arnold, J., Gao, J., 2017. Development of a station based climate database for SWAT and APEX assessments in the US. Water 9, 437. https://doi.org/10.3390/w9060437.

Yang, X., He, R., Ye, J., Tan, M.L., Ji, X., Tan, L., Wang, G., 2020. Integrating an hourly weather generator with an hourly rainfall SWAT model for climate change impact assessment in the Ru River Basin. China. Atmospheric Res. 244, 105062 https://doi.org/10.1016/j.atmosres.2020.105062.

Zhu, Q., Xuan, W., Liu, L., Xu, Y.-P., 2016. Evaluation and hydrological application of precipitation estimates derived from PERSIANN-CDR, TRMM 3B42V7, and NCEP-CFSR over humid regions in China: evaluation and Hydrological Application of Precipitation Estimates. Hydrol. Process. 30, 3061–3083. https://doi.org/10.1002/hyp.10846.